Multipole moments of ^{154}Sm, ^{176}Yb, ^{232}Th, and ^{238}U from proton inelastic scattering

C. H. King,* J. E. Finck,† G. M. Crawley, J. A. Nolen, Jr., and R. M. Ronningen
Cyclotron Laboratory, Michigan State University, East Lansing, Michigan 48824
(Received 25 June 1979)

We have measured the inelastic scattering of 35 MeV protons from the nuclei ^{154}Sm, ^{176}Yb, ^{232}Th, and ^{238}U. Angular distributions were extracted for $J^\pi = 0^+$–8^+ members of ground state rotational bands. These data were analyzed using coupled channels calculations for scattering from a deformed optical potential. Searches were made on some of the parameters of this potential, including the deformation parameters β_2 and β_4. The multipole moments of the potential distribution were calculated from the parameter values and are compared to the results of Coulomb excitation, electron scattering, and inelastic, alpha-particle scattering studies. In general, these moments deduced in our investigation agree better with those from Coulomb excitation and electron scattering than with moments deduced from α-particle scattering. But we also find the moments from our study to be systematically smaller than those from Coulomb excitation.

[NUCLEAR REACTIONS ^{154}Sm(p,p'), ^{176}Yb(p,p'), ^{232}Th(p,p'), and ^{238}U(p,p'), $E_p = 35$ MeV; enriched targets, nuclear emulsion plates (7 keV FWHM) and position-sensitive proportional counter (15 keV FWHM), magnetic spectrograph; measured $\sigma(Ep', \theta)$; coupled channels calculations, rotational model; deduced optical model and deformation parameters, quadrupole and hexadecapole moments; comparisons to Coulomb excitation, (e,e') and (α,α'), comparisons to Hartree-Fock calculations.]

I. INTRODUCTION

The shape of a nucleus is one of its most fundamental properties, but the precise determination of the nuclear shape is still an outstanding problem. The most extensive and accurate data on nuclear deformations have come from Coulomb excitation measurements. However, in practice, the information which can be obtained from such measurements is incomplete. Because of the rapid decrease of excitation probabilities for the higher-order moments, the Coulomb excitation technique is essentially restricted to determinations of quadrupole (E2) and hexadecapole (E4) moments. Even the hexadecapole moment is often difficult to obtain precisely and is subject to ambiguities. (See, for example, Ref. 1 and references cited therein.) More importantly, Coulomb excitation is sensitive only to the charge distribution of a nucleus, and although information about higher charge moments might be obtained from higher momentum-transfer Coulomb measurements, such as high-energy electron scattering, information about the neutron distribution of a nucleus requires hadronic probes.

The standard technique for investigating nuclear shapes is the measurement of inelastic scattering cross sections. However, because the nuclear interaction is poorly understood and is much more complicated than the electromagnetic interaction, it is difficult to make model-independent determinations of nuclear shapes from such measurements. For simplicity it is usual to analyze the data in terms of a parametrized deformed optical model potential[2] (DOMP), which is a complex projectile-nucleus potential as in the normal optical model but with additional parameters describing the deformation of the nuclear surface. The parameters are then adjusted to fit both the elastic and inelastic scattering cross sections. The phenomenological nature of this model makes the deformation parameters (β_λ) determined by such an analysis rather uncertain and difficult to compare with Coulomb excitation results. Recently, Mackintosh[3] has pointed out that deformed optical model potentials which are derivable from a simple folding prescription (sometimes called the reformulated optical model[4]) have the property that their multipole moments are proportional to those of the underlying matter distribution. Thus, to the extent that the DOMP satisfies this property, the moments of the mass distribution can be determined in a model-independent way.

Most of the hadron scattering data on heavy nuclei have come from measurements using complex projectiles, principally the pioneering α-scattering measurements of Hendrie et al.[5] However, protons appear to have several possible advantages over composite projectiles as probes of the neutron distribution. The parametrized optical-model potentials for α-particles are known to possess many more ambiguities than those for protons making proton scattering a more suitable candidate for the moment analysis suggested by Mackintosh. In addition, the fact that the p–n interaction is stronger than the p–p and n–n interactions makes proton scattering more sensitive to the neutron distribution. Furthermore, the higher penetrability of protons in nuclear matter allows them to probe the nuclear interior, and the electron-scattering data of Cooper et al.[6] have given preliminary indications that for some deformed nuclei the deformations in the interior may be different from those at the surface. Finally, proton scattering should lend itself more readily to more fundamental analyses such as those using folding-model potentials.

Almost all proton scattering on heavy deformed nuclei has been measured at fairly low proton energies where the angular distributions are not sufficiently diffractive to be very sensitive to nuclear deformations. The purpose of the present study is to provide higher energy (p,p') data so that the possible advantages of proton scattering as a probe of nuclear deformations can be realistically assessed. We have chosen a proton bombarding energy of 35 MeV and the targets ^{154}Sm, ^{176}Yb, ^{232}Th, and ^{238}U, all of which have been studied by both Coulomb excitation and electron scattering. For the present we have chosen to analyze the data in the usual manner with a DOMP and will try to relate the results to those from the Coulomb measurements using the multipole moment

technique suggested by Mackintosh. A preliminary report of this research has appeared elsewhere.[7]

II. EXPERIMENTAL PROCEDURE

The inelastic scattering reactions were measured using 35 MeV protons from the Michigan State University isochronous cyclotron with scattered protons detected in the focal plane of the Enge split-pole spectrometer. Two detection techniques were employed: 1) a delay-line position-sensitive proportional counter with an energy resolution of 15 keV full width at half maximum (FWHM), and 2) to obtain better resolution some data for ^{154}Sm and ^{176}Yb were recorded on photographic plates with a resolution of 7 keV FWHM. The ^{154}Sm and ^{176}Yb targets consisted of metals prepared from enriched oxides by standard lanthanide reduction techniques and were 150 μg/cm^2 of ^{154}Sm enriched to 99% and 200 μg/cm^2 of ^{176}Yb enriched to 97%. The ^{232}Th and ^{238}U targets were in the form of natural thorium and uranium tetraflourides. The ^{232}Th target was 240 μg/cm^2 thick and the ^{238}U target was 220 μg/cm^2 thick.

Data were recorded at laboratory angles from 20° to 120° in 5° steps. A monitor detector at 90° was employed to assure accurate relative normalizations. Most of these data were obtained using a spectrograph defining aperture with an angular width of 1° × 2°, but sometimes widths of 1° × 1° (at forward angles) and 2° × 2° were also used.

Proton spectra recorded on photographic plates from the lanthanide targets are shown in Fig. 1. The elastic and first excited states produce tracks too dense to scan. The 4^+, 6^+, and 8^+ states of the ground state rotational band are clearly observed. Many higher-lying levels from excited bands are also resolved and the strongest of these states are comparable in magnitude to the 6^+ state of the ground state band. Fig. 2 shows spectra of the actinide nuclei recorded with the proportional counter. The ground state band is observed up to the 10^+ state. In ^{238}U many states from excited bands are observed, and the $K^\pi J = 0^-_3$

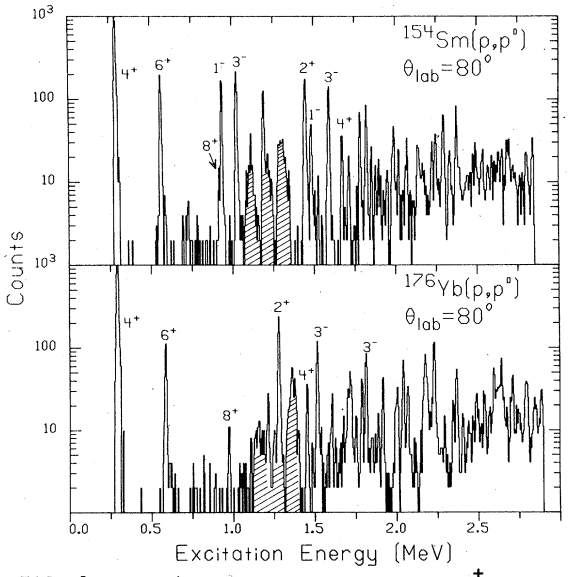

FIG. 1. Partial spectra (elastic and 2^+ excitation peaks excluded) of inelastically scattered protons from ^{154}Sm and ^{176}Yb recorded on photographic plates. The broad peaks with hatching are contaminant peaks. Some examples of peaks with known spins and parities are shown.

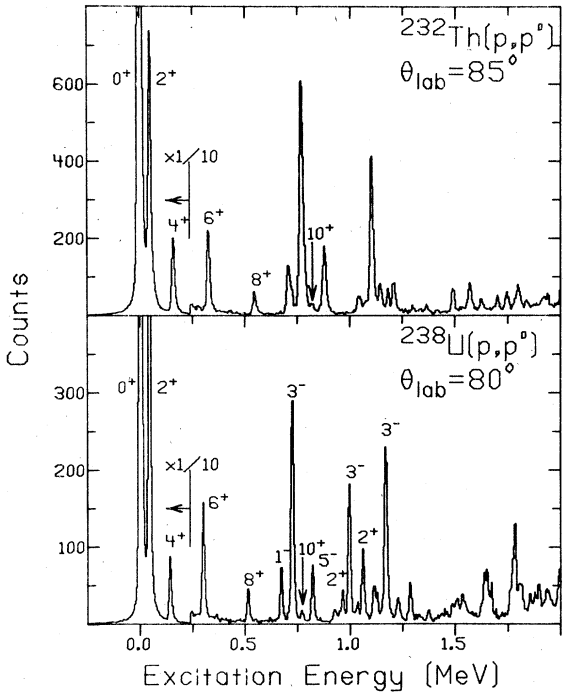

FIG. 2. Partial spectra of elastically and inelastically scattered protons from ^{232}Th and ^{238}U recorded with a proportional counter.

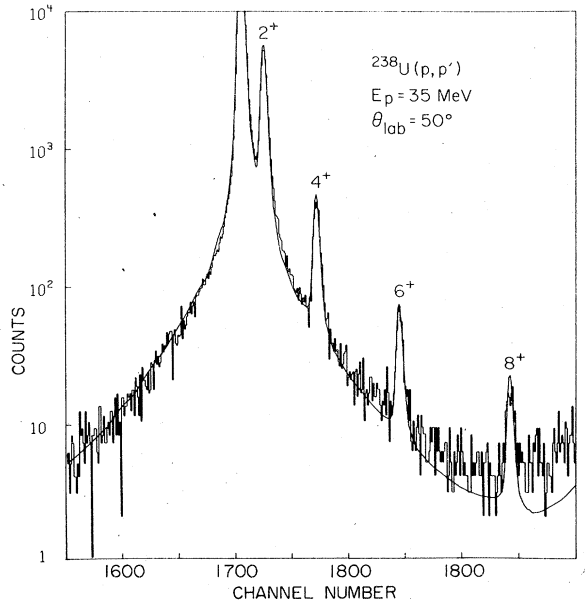

FIG. 3. An example of a fit to the ground band peaks in ^{238}U. The solid line is the result of the iterative fitting procedure described in the text. The large "wings" on the peaks are believed to result from a degradation of position resolution as delta rays are produced in the proton-gas (propane) collisions.

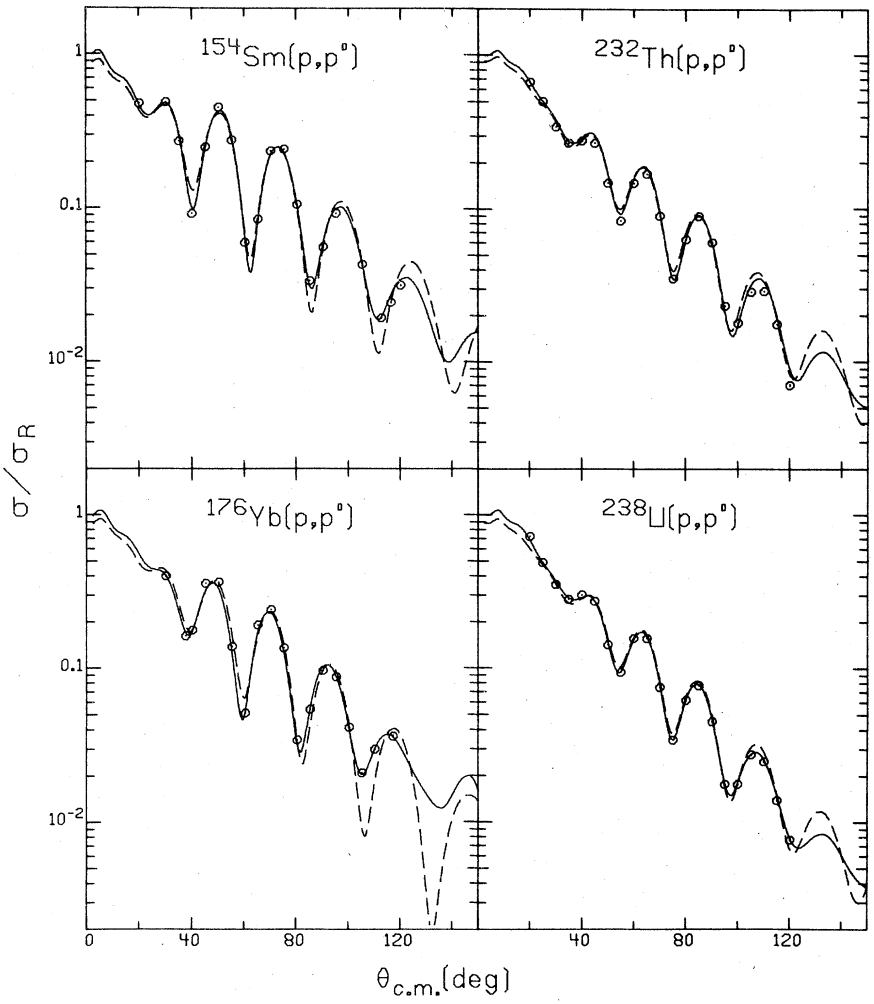

FIG. 4. Fits to the elastic scattering data. The solid line is the result of calculations employing the spin-orbit interaction. The dashed line is the result of calculations without this interaction. The data for these latter results have a somewhat different normalization so this calculation has been renormalized for display purposes to the absolute cross sections predicted by the calculations using the spin-orbit interaction. All parameters for these fits are given in Table I.

state at 0.732 MeV and the 2^-3 state at 1.169 MeV are stronger than the 6^+ member of the ground state rotational band at this angle.

In extracting cross sections, the peak shapes were assumed to be identical for all states in a particular spectrum. The peak areas were extracted by an iterative procedure based on the shape of the elastic peak with the low energy tail varied to assure a best fit for all states of interest. An example of the peak fitting results is shown in Fig. 3 for ^{238}U(p,p'). Each data point has a 3% normalization and peak stripping error added in quadrature to the statistical uncertainty.

The proton angular distributions from the ^{154}Sm, ^{176}Yb, ^{232}Th, and ^{238}U targets leading to the ground state and excited levels of the ground state rotational band are shown in Figs. 4, 5, and 6. A striking feature of the data is the oscillatory nature of these angular distributions. This is in contrast to the structureless angular distributions observed both in lower energy proton scattering on these same nuclei,[8,9] and in scattering from heavy spherical nuclei at 35 MeV.[10] A second qualitative characteristic of the data is that the magnitude of the cross sections decreases by approximately an order of magnitude for each successively higher-lying ground band state.

The absolute cross sections were inferred by comparisons of the measured elastic scattering cross sections to those predicted by the coupled channels calculations (see Sec. III).

III. ANALYSIS

The data have been analyzed in the standard manner[2,5] using a DOMP to determine the transition matrix elements. The calculations were carried out using the coupled channels code ECIS of J. Raynal.[11] It was assumed that the nuclear states are members of a K = 0 band resulting from the rotation of rigidly deformed static mass and charge distributions. All non-zero couplings to order L = 8 (to order L = 10 for investigations involving β_6 but with no spin-orbit interaction) were included in the coupled channels spaces, specified below.

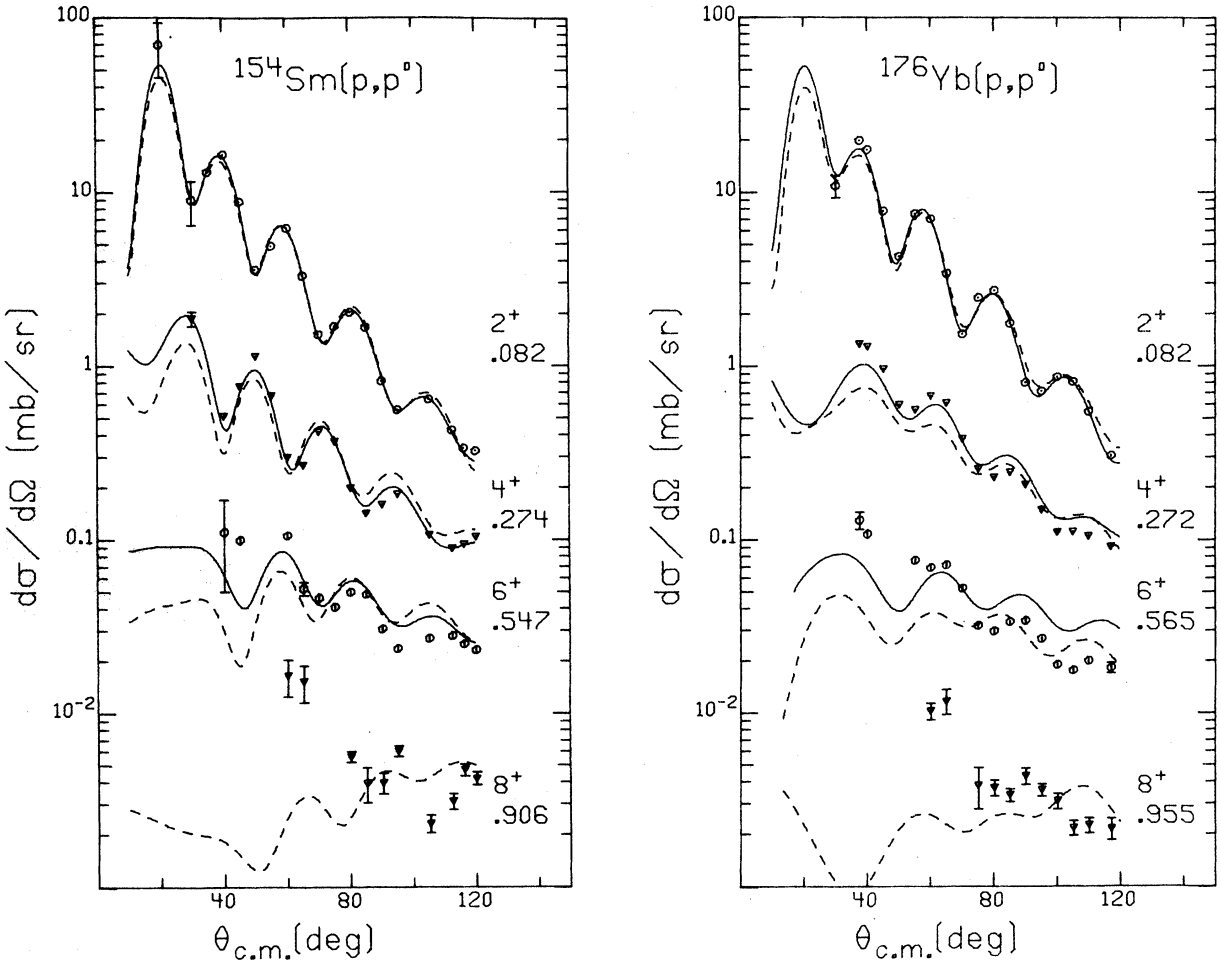

FIG. 5. Best-fit results for the inelastic scattering data for ^{154}Sm and ^{176}Yb. The solid line results from calculations employing the spin-orbit interaction, coupling all levels up to 6^+ to L = 8. The dashed lines result from calculations not employing the spin-orbit interaction, but coupling all levels up to 8^+ to L = 10. The deformation parameters used in these calculations are given in Table I.

The nuclear potential was assumed to have the standard Woods-Saxon radial dependences, with the deformations introduced by replacing the real and imaginary radii by

$$R(\theta) = r_0 A^{1/3} (1 + \sum_\lambda \beta_\lambda Y_{\lambda 0}(\theta)).$$

Only β_2 and β_4 deformations were normally used; the moments we present in Sec. IV result from these deformations only. We did extend the calculations to include β_6 in some cases (with no spin-orbit interaction) as discussed below. A uniform but deformed Coulomb potential was employed with the values of the charge deformation parameters β_2^c and β_4^c taken to be those which reproduce the charge distribution moments deduced in Coulomb excitation studies (Ref. 12 and see survey in Ref. 1). All calculations employed 25 partial waves with integrations carried out to 20 fm.

There is a substantial amount of coupling between the deformation parameters. That is, direct and multistep processes compete strongly, especially for the 4^+ and higher state excitations. As shown in Fig. 7 for ^{176}Yb, the 4^+ and 6^+ angular distributions are very sensitive to both the sign and the magnitude of β_4. This is especially encouraging as the region of Yb, Hf, and W is the subject of recent attention (e.g. Ref. 13) as to the magnitude of hexadecapole effects there.

In order to reduce the number of parameters which might be varied to fit the data, the initial calculations for the elastic scattering data were started with the spherical average optical model parameters of Becchetti and Greenlees.[14] By means of gradient searching, including the 0^+, 2^+, and 4^+ states, the real well depth V, the imaginary surface well depth W_d, and the real and imaginary diffusenesses, a_r and a_i, were adjusted to give best fits (minimum χ^2 values) to the elastic angular distribution. These searches were iterated with initial searches on the deformation parameters, as the calculations obviously depend on them as well as the "geometrical" parameters.

We approached the problem of spin-orbit effects by analyzing the data with and independently without the inclusion of the spin-orbit interaction. We used a deformed, full-Thomas form (c.f. Ref. 15) for this interaction, which gave good fits over our angular range. For simplicity, we kept all deformations equal for the nuclear part of the optical potential, including the spin-orbit part. Only its depth V_{so} was adjusted and average

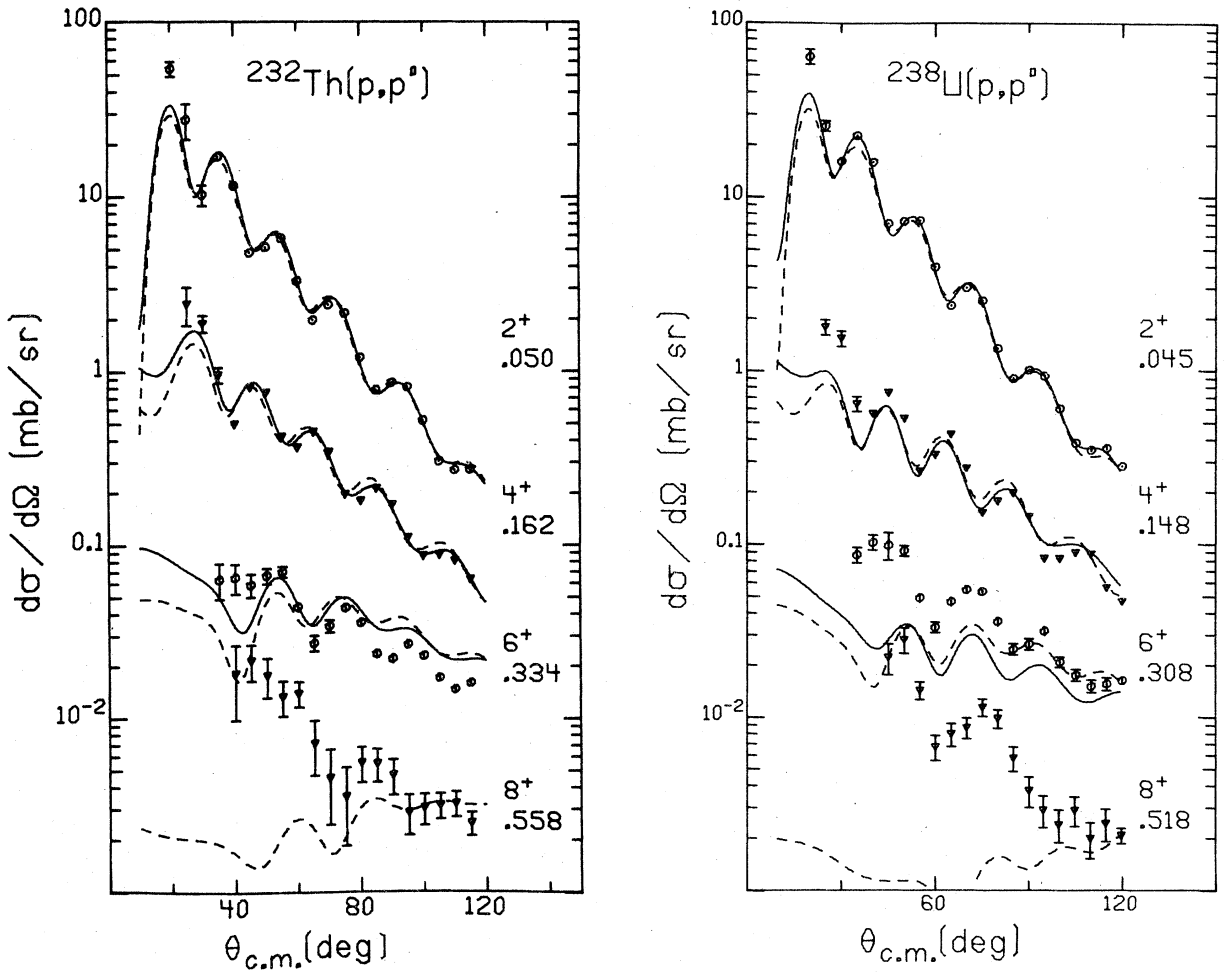

FIG. 6. Best-fit results for the inelastic scattering data for ^{232}Th and ^{238}U. See the caption for Fig. 5 for description of the curves.

radius and diffuseness values[14] were used.

The best fit results for the elastic scattering data are shown in Fig. 4 for calculations with and without the spin-orbit interaction. We tabulate the resulting optical model parameter values in Table I. Note in Fig. 4 that the inclusion of the spin-orbit interaction is necessary to properly describe the minima, most noticeably for ^{176}Yb. Without including the spin-orbit term the imaginary surface depth W_d must be greatly increased in order to decrease the depths of these minima from the extremely deep ones which result if one uses the spherical, average parameters.[14]

The procedure for fitting the inelastic scattering data was typically as follows. By grid-searches, including the 0^+, 2^+, and 4^+ states, β_2 was varied, assuming some fixed, "reasonable" β_4 value, to best fit the 2^+ angular distribution. Using the resulting β_2 value β_4 was similarly determined, but with the coupled channels space increased to include the 6^+ state (and sometimes the 8^+ state if no spin-orbit interaction was employed). These two steps were iterated, attempting to minimize the χ^2 values for each angular distribution (χ^2_{0+}, χ^2_{2+}, and χ^2_{4+}) at consistent values of β_2 and β_4. Unique values of β_2 and β_4 will minimize the χ^2 values (within $\pm$20%) for the 0^+, 2^+, and 4^+ states, but not for the 6^+ states. In choosing "best" values of β_2 and β_4, those given in Table I, we took those which minimized the total χ^2 value, taken to be the sum of χ^2_{0+}, χ^2_{2+}, and χ^2_{4+} (we omit χ^2_{6+} because β_6 deformations were not included). An example of the χ^2 values as functions of β_2 and β_4 for ^{238}U is shown in Fig. 8. In the case of ^{176}Yb, however, χ^2_{0+} and χ^2_{2+}, but not χ^2_{4+}, will minimize at very nearly the same value of β_2. Minimizing χ^2_{4+} with respect to β_2 will typically cause increases of 20%–30% in χ^2_{0+} and χ^2_{2+} from the values minimized with respect to β_2. In this case the best β_2 value is taken as that for which χ^2_{0+} and χ^2_{2+} are at a minimum, and β_4 is that value for which χ^2_{4+} is minimized.

The inclusion of β_6 was investigated (these calculations could only be done without the spin-orbit interaction, but the 8^+ state and couplings to L = 10 were included). However, the fits of the 6^+ angular distributions remained poor for those values of β_6 ($|\beta_6| \approx 0.015$) which would help minimize the total χ^2 (here, χ^2_{6+} was included). We cannot then conclude anything definite about β_6 values for those nuclei. Such small values of β_6 do not affect within uncertainties the quadrupole and hexadecapole moments that we report.

The statistical uncertainties in β_2 and β_4 were obtained by gradient searches using the automatic searching routine of ECIS. These uncertainties are derived from the inverse of the matrix of second

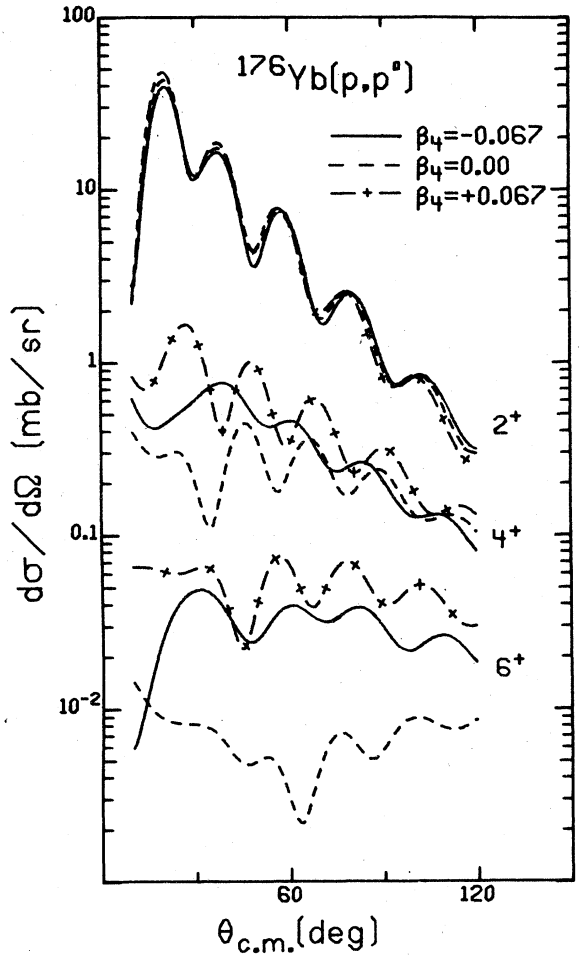

FIG. 7. Sensitivity of the calculations to the sign and magnitude of β_4 for ^{176}Yb.

derivatives of χ^2 with respect to the varied deformation parameters, and account for correlations between these parameters.

IV. DISCUSSION

It is clear that the deformation parameters β_λ obtained from a DOMP analysis of inelastic hadron scattering are subject to the same ambiguities of interpretation as the more ordinary optical model parameters. For one thing, since the inelastic scattering cross sections depend on β_λ only through the product $R\beta_\lambda$ (where R is the potential radius), the value of β_λ is entirely dependent on the choice of R. Hence, it is clear that the "deformation length" $\delta_\lambda \equiv R\beta_\lambda$ is a more fundamental quantity, and it is common to compare the results of different experiments by comparing the deduced δ_λ. However, this procedure ignores the correlations between the β_λ and the remaining optical model parameters and is completely inadequate for comparing hadron scattering with Coulomb measurements, since unlike the hadron-scattering cross sections, the Coulomb cross sections do not depend simply on the δ_λ. As a result, Hendrie[16] has suggested a simple geometrical construction for relating potential and matter distributions. To achieve this, he assumed that the projectile is a hard sphere, that the nuclear surface is sharp, that the projectile does not penetrate the nuclear surface, and that the difference between the potential and matter distributions is entirely due to the size of the projectile. However, the significance of this model is open to question, since it ignores not only the nuclear and projectile diffuseness and interpenetration, but also the finite range of the nucleon-nucleon interaction and the difference between its isoscalar and isovector components.

In order to avoid such problems resulting from direct comparisons of deformation parameters, deformation lengths, or geometrically scaled parameters, we have followed the suggestion of Mackintosh[3] and computed the potential multipole moments q_λ:

$$q_\lambda = \frac{K\int V(r-R(\theta))r^{\lambda+2}Y_{\lambda 0}(\theta)d\theta\,dr}{\int V(r-R(\theta))r^2 d\theta\,dr}$$

Table I. Optical model parameters for coupled channels calculations.

		V^a (MeV)	a_r (fm)	W_d^b (MeV)	a_i (fm)	V_{so}^c (MeV)	β_2	β_4
^{154}Sm	d	50.70	0.729	5.113	0.686	6.330	0.269 (3)	0.072 (3)
	e	49.80	0.667	8.392	0.604		0.273 (5)	0.066 (5)
^{176}Yb	d	52.45	0.705	4.204	0.738	6.430	0.275 (4)	-0.055 (4)
	e	49.67	0.652	7.745	0.653		0.277 (7)	-0.066 (6)
^{232}Th	d	52.72	0.716	5.086	0.788	5.513	0.210 (3)	0.069 (3)
	e	51.70	0.707	7.085	0.759		0.211 (4)	0.071 (3)
^{238}U	d	53.59	0.732	4.331	0.810	6.776	0.232 (3)	0.042 (3)
	e	52.15	0.653	6.121	0.789		0.233 (4)	0.049 (5)

[a]The real radius was kept fixed at r_r = 1.17 fm.

[b]The imaginary radius was kept fixed at r_i = 1.32 fm.

[c]The spin-orbit geometry parameters were kept fixed at r_{so} = 1.01 fm and a_{so} = 0.705 fm.

[d]These parameters resulted from best-fits for calculations which included the spin-orbit interaction.

[e]These parameters resulted from best-fits for calculations not employing a spin-orbit interaction.

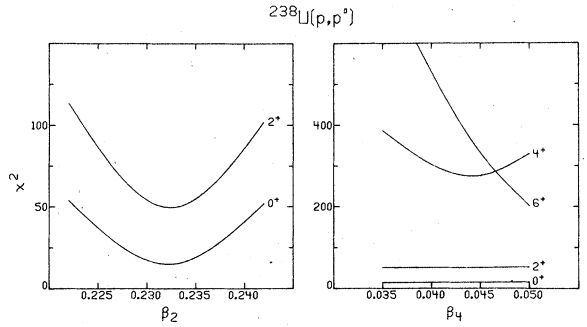

FIG. 8. Plots of the χ^2 values for angular distribution data vs. a) β_2 and b) β_4 for ^{238}U (spin-orbit interaction included in the calculations). Note that the 6^+ data is not minimized at consistant values of β_2 and β_4 as the other data are. In these calculations $\beta_6 = 0$ but the situation is only little improved by any other value.

where V(r-R(θ)) is the real part of the DOMP and K is a normalization constant. Mackintosh has shown[3] using a theorem due to Satchler[17] that for a folding-model potential in which the underlying nucleon-nucleon interaction is assumed to depend only on the magnitude of the distance between the nucleons in the projectile and target (reformulated optical model) the multipole moments of the potential (q_λ) are proportional to those of the nuclear density. Thus, to the extent that our DOMP is equivalent to such a reformulated optical-model potential, the q_λ we calculate should be proportional to the nuclear density moments. In particular, if the neutron and proton distributions are the same and the normalization constant K is chosen to be equal to Z, the atomic number, the q_λ we measure should be equal to the charge moments measured by Coulomb techniques. Therefore, to facilitate comparison with Coulomb measurements, we have chosen K = Z so that the q_λ may be considered to be the "charge-component" moments of the potential.

The q_2 and q_4 calculated in this manner from the DOMP parameters given in Table I are shown in Table II. Also shown are the moments deduced from (α,α') studies[5,16,18] and charge moments from Coulomb excitation (Ref. 1 and references cited therein) and electron scattering measurements. In the electron scattering measurements of Cooper et al.[6] the quadrupole moment (q_2) is not determined but instead is taken from Coulomb excitation B(E2) measurements. Thus, the q_2 values used in (e,e') are not shown in Table II. In addition, as indicated in Table II, only the magnitude and not the sign of the hexadecapole moments (q_4) could be obtained from these (e,e') measurements. It should also be noted that for the case of ^{238}U the value of B(E2) (11.70(15)e^2b^2) used by Cooper et al. is a more preliminary value of the one measured by Bemis et al.[12] (12.30(15)e^2b^2).

A comparison of the results shown in Table II indicates that the potential moments derived from our fits generally agree better with the charge moments from Coulomb excitation and electron-scattering measurements than with (α,α') results. In fact, our moments and the electromagnetic moments are consistently smaller than the (α,α') moments with the one exception of the ^{238}U measurement of David et al.[18] (It is also worth noting that there is a significant difference between the two (α,α') results quoted for ^{238}U.) The discrepancy between moments from α-particle scattering and those from Coulomb measurements has been noted also by Mackintosh[3] and may indicate that the α-scattering potentials used are not derivable from reformulated

Table II. E2 and E4 moments in ^{154}Sm, ^{176}Yb, ^{232}Th, and ^{238}U.

Nuclide	Method	q_2 [a] (b) or (eb)	q_4 [a] (b^2) or (eb^2)
^{154}Sm	(p,p') at 35 MeV[b]	2.06 (3)	0.54 (2)
	Coulomb excitation[c]	2.094 (4)	0.588 (29)
	(e,e')[d]		|0.47| (1)
	(α,α') at 50 MeV[e]	2.38	0.61
^{176}Yb	(p,p') at 35 MeV[b]	2.29 (5)	-0.09 (3)
	Coulomb excitation[c]	2.325 (18)	0.28 ($\frac{11}{20}$)
	(e,e')[d]		|0.10|
	(α,α') at 50 MeV[e]	2.76	-0.17
^{232}Th	(p,p') at 35 MeV[b]	2.93 (6)	0.98 (5)
	Coulomb excitation[f]	3.03 (1)	1.22 (15)
	(e,e')[d]		|1.08| (2)
	(α,α') at 50 MeV[g]	2.97 (21)	1.06 (20)
^{238}U	(p,p') at 35 MeV[b]	3.30 (6)	0.81 (6)
	Coulomb excitation[f]	3.51 (2)	0.83 (22)
	(e,e')[d]		|1.10| (3)
	(α,α') at 50 MeV[g]	2.98 (12)	0.74 (8)
	(α,α') at 50 MeV[h]	3.75 (22)	1.42 (27)

[a] The units for the charge component moments are b^λ, λ = 2 or 4. The units for the electromagnetic moments are eb^λ.

[b] Present work using the values of the parameters in Table I with spin-orbit interaction. Calculations without spin-orbit interaction yield the following changes in q_2: −0.01, −0.03, +0.01, and −0.01 b, and in q_4: −0.05, −0.04, +0.02, +0.03 b^2 for ^{154}Sm, ^{176}Yb, ^{232}Th, and ^{238}U, respectively.

[c] The Coulomb excitation values for q_2 and q_4 are results of the survey of Ref. 1.

[d] Ref. 6. "||" denotes the absolute value of the enclosed number.

[e] Ref. 5.

[f] Ref. 12.

[g] Ref. 18.

[h] Ref. 16.

Table III. Quadrupole and hexadecapole moments from the density dependent Hartree-Fock calculations by Negele and Rinker.[a] Moments for both the proton (p) and neutron (n) densities are given.

	q_2^p (b)	q_2^n (b)	q_4^p (b^2)	q_4^n (b^2)
^{154}Sm	2.02	1.96	0.41	0.45
^{176}Yb	2.49	2.46	0.057	0.049
^{232}Th	2.63	2.78	0.84	0.92
^{238}U	3.29	3.38	1.01	1.02

[a]To make comparisons with our results the results of Negele and Rinker[19] are multiplied by $[(2\lambda + 1)/16\pi]^{1/2}$ for both proton and neutron moments, and the neutron moments are further multiplied by Z/N.

optical-model potentials so that these (α,α') results may not be useful measurements of the nuclear deformations.

Although our potential moments generally agree quite well with the measured charge moments, the values are systematically lower. For the quadrupole moments this difference is only statistically significant for ^{232}Th and ^{238}U, becoming as large as 6% in the case of ^{238}U. The largest discrepancy in the hexadecapole moments is for ^{176}Yb, in this case the Coulomb values are quite uncertain and our values are problematic as well, due to the difficulties experienced in fitting described in Sec. III. For ^{238}U, it is difficult to assess the apparent discrepancy between the value of q deduced in our work and the value from electron scattering because of the value of B(E2) chosen in Ref. 6 mentioned above. Despite such considerations, the systematic nature of the discrepancies (proton-scattering results always smaller than Coulomb results) for all cases is perhaps significant.

If these discrepancies are taken seriously, they mean that in the cases we have studied the neutron moments are smaller than the proton moments. Microscopic calculations of neutron and proton moments for heavy nuclides have recently been performed by Negele and Rinker[19] using the density-dependent Hartree-Fock formalism with a "realistic" nucleon-nucleon interaction (Reid soft-core potential). Their results for the nuclides studied in this work are shown in Table III and indicate that differences as large as 5% between proton and neutron quadrupole moments are predicted. However, in the cases of ^{232}Th and ^{238}U, for example, our differences are of the opposite sign to those listed in Table III.

It must be emphasized, however, that at present our analysis is phenomenological. We have tried to minimize the effects of this by our multipole-moment treatment of the results. However, the validity of this treatment presupposes that our DOMP's are derivable from reformulated optical-model potentials. As indicated above, it is likely that the α-particle potentials that have been used probably do not satisfy this condition because of the large discrepancy seen between the moments derived from such potentials and the proton and Coulomb moments. It is also possible that the remaining discrepancy between the proton and Coulomb moments is also due to this fact. Some support for this possibility has been given by Hamilton and Mackintosh,[20] who have pointed out that density-dependent effects may be important. However, calculations they have performed[20] indicate that for equal neutron and proton deformations the inclusion of such effects would tend to make the potential moments larger than the charge moments, an effect opposite to our observations. Clearly, further investigations of these effects are needed.

Another uncertainty concerns the effect of the imaginary part of the DOMP. As mentioned in Sec. III, we have for simplicity set the deformation parameters equal for all parts of the potential. However, as indicated above, it is the product $R\beta_\lambda = \delta_\lambda$ which determines the scattering cross sections. If R is significantly different between the real and imaginary parts of the potential, it might be a better criterion to keep the δ_λ equal[21] between the real and imaginary parts of the DOMP. Another possible condition[22] is that the multipole moments of the real and imaginary parts be kept equal. The effect on the results of such alternative conditions needs to be considered before any final conclusions can be drawn from our results.

An additional consideration which affects not only our results but also the Coulomb measurements is the validity of the strict rotational model in determining the transitional probabilities. It is possible, for example, that a breakdown in this model accounts for the difficulties we experienced in fitting the ^{176}Yb cross sections. This may be related to similar problems observed in electron scattering. Cooper et al.[6] found it impossible to fit their ^{176}Yb cross sections unless they adjusted the deformation parameters for different transitions. They interpreted this in terms of radius-dependent deformations in the charge density, although it would seem that deformations which change as the rotational angular momentum is increased might be an equally valid interpretation. But, Coulomb excitation studies[23] of ^{176}Yb with heavy ions, to spin 18^+, show the moments-of-inertia to be smoothly varying with spin, and the lifetimes of the states to 14^+ are in agreement with rotational model predictions.

V. SUMMARY

We have measured cross sections for proton inelastic scattering on ^{154}Sm, ^{176}Yb, ^{232}Th, and ^{238}U and have fit them using a parametrized DOMP. The results have been interpreted in terms of a multipole-moment analysis, a procedure which we believe to be more fundamental than the usual one of comparing deformation parameters, deformation lengths, or geometrically scaled parameters. We found that in contrast to the α-scattering results, there is reasonable agreement with the Coulomb measurements, except that the proton moments are systematically ($\lesssim$6%) lower. If this is a significant discrepancy, it would imply systematically smaller neutron than proton moments in disagreement with Hartree-Fock calculations.[19]

However, it is probably more likely that the differences between our measured proton-scaling moments and the charge distribution moments result from the phenomenological aspects of our analysis and could be due to such things, discussed in Sec. IV, as density-dependent effects in the optical-model potential, uncertainties in the treatment of the imaginary part, and breakdown of the simple rotational model for determining the transition probabilities. It is interesting that if the first of these effects is important, the calculations of Hamilton and Mackintosh[20] indicate that its influence on the potential moments would lead to a discrepancy with the charge moments opposite to that which we observe.

All of these effects need to be examined more closely before definite conclusions can be drawn. Nevertheless, the present results indicate that proton scattering is indeed a useful hadronic probe of nuclear deformations

and demonstrate the advantages of the multipole-moment method for interpreting the results.

ACKNOWLEDGMENTS

This material is based upon work supported by the National Science Foundation under Grant No. Phy-7822696.

We wish to express our gratitude to Dr. R.S. Mackintosh for his interest in our study, and for his very helpful discussions with us. We are indebted to Dr. J. Raynal for the coupled channels code ECIS, and for communications pertaining to its use.

---

*Present address: Lawrence Berkeley Laboratory, University of California, Berkeley, CA 94720.

†Present address: Physics Department, Northern Michigan University, Marquette, MI 49855.

[1]R.M. Ronningen et al., Phys. Rev. C16, 571 (1977).

[2]See, for example, N.K. Glendenning, in Nuclear Structure and Nuclear Reactions, Proceedings of the International School of Physics, "Enrico Fermi," Course 40, edited by M. Jean and R.H. Ricci (Academic, New York, 1969), p. 232.

[3]R.S. Mackintosh, Nucl. Phys. A266, 379 (1976).

[4]G.W. Greenlees, W. Makofske, and G.J. Pyle, Phys. Rev. C1, 1145 (1970) and references therein.

[5]D.L. Hendrie et al., Phys. Lett. 26B, 127 (1969).

[6]T. Cooper et al., Phys. Rev. C13, 1083 (1976).

[7]C.H. King, G.M. Crawley, J.A. Nolen, Jr., and J. Finck, J. Phys. Soc. Japan 44, Suppl. pp. 564-569(1978).

[8]P. Stoler, M. Slagowitz, W. Makofske, and T. Kruse, Phys. Rev. 155, 1334 (1967).

[9]H.B. Kurepin, H. Schulz, and H.J. Wiebicke, Nucl. Phys. A189, 257 (1972).

[10]W.T. Wagner, G.M. Crawley, and G.R. Hammerstein, Phys. Rev. C11, 486 (1975); W.T. Wagner, G.M. Crawley, G.R. Hammerstein, and H. McManus, Ibid. 12, 757 (1975).

[11]J. Raynal, Program ECIS (unpublished).

[12]C.E. Bemis, Jr. et al., Phys. Rev. C8, 1466 (1973).

[13]R.M. Ronningen et al., Phys. Rev. Lett. 40, 364 (1978).

[14]F.D. Becchetti, Jr. and G.W. Greenlees, Phys. Rev. 182, 1190 (1969).

[15]R. de Swiniarski, Dinh-Lien Pham, and G. Bagieu, Can. J. Phys. 55, 43 (1977).

[16]D.L. Hendrie, Phys. Rev. Lett. 31, 478 (1973).

[17]G.R. Satchler, J. Math. Phys. (N.Y.) 13, 1118 (1972).

[18]P. David et al., Z. Phys. A278, 281 (1976).

[19]J.W. Negele and G. Rinker, Phys. Rev. C9, 1499 (1977); J.W. Negele, private communication.

[20]J.K. Hamilton and R.S. Mackintosh, J. Phys. G3, L19 (1977); 4, 579 (1978).

[21]See, for example, R.J. Ascuitto, C.H. King, L.J. McVay, and B. Sørensen, Nucl. Phys. A226, 454 (1974).

[22]R.S. Mackintosh, private communication.

[23]D. Ward et al., Nucl. Phys. A266, 194 (1976).